The Protein Journal (2023) 42:14–23
https://doi.org/10.1007/s10930-022-10087-0

Enzymatic Characterization and Coenzyme Specificity Conversion of a Novel Dimeric Malate Dehydrogenase from *Bacillus subtilis*

Ya-Dong Ge[1] · Yi-Tian Guo[1] · Lu-Lu Jiang[1] · Hui-Hui Wang[1] · Shao-Lin Hou[1] · Feng-Zhi Su[1]

Accepted: 14 December 2022 / Published online: 19 December 2022

Abstract
Malate is an important material to various industrials and clinical applications. *Bacillus subtilis* is a widely used biocatalyst tool for chemical production. However, the specific enzymatic properties of malate dehydrogenase from *Bacillus subtilis* (BsMDH) remain largely unknown. In the present study, BsMDH was cloned, recombinantly expressed and purified to test its enzymatic properties. The molecular weight of single unit of BsMDH was 34,869.7 Da. Matrix-Assisted Laser-Desorption Ionization-Time-of-Flight Mass Spectrometry and gel filtration analysis indicated that the recombinant BsMDH could form dimers. The k_{cat}/K_m values of oxaloacetate and NADH were higher than those of malate and NAD^+, respectively, indicating a better catalysis in the direction of malate synthesis than the reverse. Furthermore, six BsMDH mutants were constructed with the substitution of amino acids at the coenzyme binding site. Among them, BsMDH-T7 showed a greatly higher affinity and catalysis efficiency to NADPH than NADH with the degree of alteration of 2039, suggesting the shift of the coenzyme dependence from NADH to NADPH. In addition, BsMDH-T7 showed a relatively lower K_m value, but a higher k_{cat} and k_{cat}/K_m than NADPH-dependent MDHs from *Thermus flavus* and *Corynebacterium glutamicum*. Overall, these results indicated that BsMDH and BsMDH-T7 mutant might be promising enzymes for malate production.

Keywords *Bacillus subtilis* · Malate dehydrogenase · Enzymology · Coenzyme specificity conversion · Molecular evolution

1 Introduction

Malate dehydrogenase (MDH, EC 1.1.1.37) is an important enzyme in organisms, mainly catalyzing the interconversion of malate and oxaloacetate (OAA) [1], which is a rate-limiting step in the tricarboxylic acid cycle (TCA). In addition, MDH plays essential roles in diverse metabolic pathways, including gluconeogenesis, lipogenesis, protection against oxidative stress, and substrate channeling [2–5]. Moreover, MDH was developed as a biomarker for molecular breeding [6], and a potential diagnosed antigen for vaccine development [7].

In various species, MDHs with different amino acid sequences and secondary structures have been reported, displaying diverse enzymatic efficiency and affinity to substrates. Generally, MDH shows a highly conserved 3-dimensional structure, existing in the forms of dimer or tetramer. MDHs from most Gram-negative bacteria and all eukaryotes are dimeric with the molecular weights ranging from 30 to 38 kDa for each subunit. In most Gram-positive bacteria and archaea, MDHs form tetramers (130–172 kDa) [5]. According to coenzyme specificity, MDHs are divided into NAD^+-dependent (EC 1.1.1.37) and $NADP^+$-dependent types (EC 1.1.1.82). Almost all MDHs from bacteria, eukaryotic cytoplasm and mitochondria are NAD^+-dependent, while those from eukaryotic chloroplast are $NADP^+$-dependent [5].

Malate is a widely used chemical in cosmetic, textile and food industries, rapid clinical diagnostic assays (aspartate aminotransferase activity and serum bicarbonate level), and the bioremediation of heavy metal pollution [8, 9]. One efficient way to produce malate is microbial fermentation, during which MDH is the key factor determining the production efficacy and cost. For example, *Aspergillus flavus* is a well-known malate producer. It can ferment glucose to malate with a relatively high yield, but the by-product aflatoxin needs additional costs to remove [10]. The transgenic *Escherichia coli* strain with restructured malic enzymes could produce 1.41 mol of malate based on 1 mol of glucose,

✉ Ya-Dong Ge
geyd@ahnu.edu.cn

[1] College of Life Sciences, Anhui Normal University, Wuhu 241000, People's Republic of China

and accumulate 34 g/L malate in the culture media [11]. The transgenic *Bacillus subtilis* strain with phosphoenolpyruvate carboxylase and malate dehydrogenase from *Saccharomyces cerevisiae* further increased malate production [12]. Although industrial production of malate using MDH activity-enhanced bacteria have been realized, further exploration of MDH from other species may provide more choices for industrial production of malate.

Bacillus subtilis is a promising biocatalyst platform, due to its well-characterized genetic background, mature fermentative technology, and high tolerance to solvent and environmental stresses owing to its thicker cell wall compared with other microorganisms [13–17]. In addition, *B. subtilis* expresses various enzymes including proteases, cellulases, xylanases and amylases. Thus, it can utilize a wide range of carbon and energy sources. Thus, based on some cheaper substrates, *B. subtilis* may be used to produce malate [18–20]. However, up to date, the specific enzyme properties of *B. subtilis* MDH (BsMDH) has not yet been reported, which are important basic information for further development of *B. subtilis* as a malate production tool. In addition, all bacterial MDHs require NAD^+ as the coenzyme. Thus, the yield of malate partially relies on the speed of NAD^+ regeneration. To resolve this question, one strategy is the enhancement of coenzyme regeneration mechanism. For example, Lu and Mei [21] enhanced coenzyme formation mechanisms in *E. coli*, which effectively elevated the overall efficacy of $NADP^+$-dependent enzymes. Alternatively, switch of the coenzyme specificity from insufficient coenzyme to abundant coenzyme by mutation of the coenzyme binding sites might also increase the final efficacy of coenzyme-dependent enzymes. Following this thought, mutation of the NAD^+-binding site in BsMDH to NADP+-binding sequence might create novel NADP+-dependent bacterial MDHs, which might contribute more selections for industrial applications.

In this study, we cloned, recombinantly expressed and purified BsMDH. Next, its enzymatic properties were characterized. Moreover, to create more MDHs with different properties, the coenzyme binding sites of BsMDH were mutated and their specificity to coenzymes were tested. Overall, these results would contribute more MDH protein sequences for industrial applications and also promote our understanding of MDH functions in *B. subtilis*.

2 Materials and Methods

2.1 Gene Cloning

Bacillus subtilis ATCC 6051 was purchased from the China General Microbiological Culture Collection Center (CGMCC). Genomic DNA was extracted using a bacterial genomic DNA rapid extraction kit (Protein Biotech, Beijing, China). The *BsMDH* gene (GenBank accession number NC020507.1) was amplified using 2×Pfu PCR Master Mix (Protein Biotech, Beijing, China) with primers, 5′-AAA ATGTGCATATGATGGGAAATACTCGT-3′ and 5′-AGC CGCTCGAGTTAGGATAATACTTTCA-3′. Next, the PCR product was ligated to the pET- 28b(+) plasmid using the restriction enzymes *Nde* I and *Xho* I (New England BioLabs Inc., UK). The vector was transformed into *E. coli* DH5α. After DNA sequencing, the correct recombinant plasmid was extracted.

MEGA 7.0 was used to construct the phylogenetic tree of BsMDH and other MDHs with 1000 bootstraps [22]. Sequence alignment was conducted using Clustal W [23]. Prediction of secondary structure was conducted using the PSIPRED 4.0 tool online (http://bioinf.cs.ucl.ac.uk/psipred/).

2.2 Protein Expression and Purification

The recombinant plasmid was transformed into *E. coli* Rosetta BL21(DE3) pLysS and a positive clone was cultured overnight at 37 °C in LB medium containing 30 mg/L kanamycin (Macklin, Shanghai, China) and 30 mg/L chloramphenicol (Macklin, Shanghai, China). Next, *E. coli* was inoculated into fresh LB medium. When the OD_{600nm} reached 0.4–0.6, 0.5 mM IPTG (Macklin, Shanghai, China) was added and then further cultured at 20 °C for 20 h. *E. coli* cells were harvested by centrifugation at 5000 rpm for 20 min, and then suspended in 20 mL of LEW buffer (50 mM NaH_2PO_4, 300 mM NaCl, pH 8.0). Cells were homogenized by ultrasonication for 40 min on ice (20 s for sonication and 40 s for cooling, 40 cycles). After centrifugation at 10,000 rpm and 4 °C for 20 min, his_6-tagged target proteins in the supernatant were purified using the Co^{2+}-affinity chromatography (Genscript, Nanjing, China) at 4 °C. The obtained protein was visualized by the sodium dodecyl sulfate polyacrylamide gel electrophoresis (SDS–PAGE).

2.3 Molecular Mass Determination

Protein concentration was determined using a Quick Start Bradford protein assay kit (Bio-Rad, Irvine, USA) with bovine serum albumin (BSA) as the standard, and approximately 2.5 mg of BsMDH in total was analyzed using gel filtration for preliminary molecular calculation. After treatment with thrombin (Macklin, Shanghai, China), the BsMDH without his_6-tag was visualized on native PAGE, and its molecular weight was determined using a Matrix-Assisted Laser-Desorption Ionization-Time-of-Flight Mass Spectrometry (MALDI-TOF MS) 5800 Analyzer (AB SCIEX, USA) as previously described [24]. Briefly, 0.6 µl of sample was mixed directly onto the target plate with the

matrix solution (1:3 vol/vol), air-dried and then measured usign the machine. The mass spectrometry data have been deposited to the figshare (https://doi.org/10.6084/m9.figshare.13525388). Moreover, a Gel Permeation Chromatography coupled to Multi-Angle Light Scattering (GPC-MALS, Wyatt Technology Co., USA) system was also employed to detect the molecular weight of BsMDH.

2.4 Determination of Enzyme Activity and Kinetic Properties

The enzymatic properties of the recombinantly expressed protein were determined as follows. MDH catalyzes the reversible transformation from oxaloacetate (OAA) and NAD(P)H to malate and $NAD(P)^+$. Since NAD(P)H has a characteristic absorption at 340 nm, the enzyme activity can be calculated by monitoring the change of $OD_{340\ nm}$. The reaction system contained 100 mM Tris–HCl (pH 8.0), 2.25 mM OAA and 0.25 mM NAD(P)H. The standard reaction solution was thoroughly mixed with the appropriate amount of enzyme solution and then maintained at 25 °C for 60 s. The reduction of NAD(P)H per unit time was measured by monitoring the absorbance at 340 nm using a Cary 300 Bio UV–Visible spectrophotometer (Varian, CA, USA). Enzyme activity was expressed as micromoles of NADH oxidized/NAD^+ reduced per minute of reaction time per milliliter of enzyme solution [25]. Substrate kinetics and coenzyme kinetics, including K_m values for oxaloacetate, L-malate, NADH, and NADPH were determined. K_m, k_{cat} and k_{cat}/K_m were estimated based on the Michaelis–Menten plots. All experiments were conducted in triplicates independently.

2.5 Effects of pH and Temperature on Enzyme Activity

To determine the effects of pH and temperature on the enzymatic activity of BsMDH, the pH of the reaction solution was adjusted from 7.0 to 9.0 at the interval of 0.5, and the temperature was adjusted from 20 to 55 °C at the interval of 5 °C. The BsMDH activity was assessed as described above. To investigate the thermal stability of BsMDH, enzyme solution was incubated at different temperatures (from 30 to 55 °C at the interval of 5 °C) for 20 min, placed in an ice bath for 5 min and then the enzyme activities were determined at 25 °C.

2.6 Effects of Metal Ions and Compounds on Enzyme Activity

The monovalent metal ions (K^+, Na^+, Rb^+ and Li^+) and divalent ions (Mn^{2+}, Mg^{2+}, Co^{2+}, Ca^{2+}, Zn^{2+}, Cu^{2+} and Ni^{2+}) at a final concentration of 2 mM were added into the reaction system according to methods described previously [26], and then BsMDH activity was measured as described above. Similarly, the effects of three kinds of purine nucleotides (adenosine triphosphate, adenosine diphosphate and Adenosine monophosphate, abbreviated as ATP, ADP and AMP) and three kinds of metabolic compounds (α-ketoglutarate, dithiothreitol, and ethylene diamine tetraacetic acid, abbreviated as α-KG, DTT and EDTA) on BsMDH activity were also analyzed. Considering as the wide application in buffer systems, the effects of DTT and EDTA were tested at two concentrations.

2.7 Construction and Expression of BsMDH Mutants

According to the known coenzyme binding site of $NADP^+$-dependent chMDH, the NAD^+ coenzyme binding site ($D^{36}IPQLEN^{42}$) in BsMDH was replaced with the amino acid sequence of $NADP^+$ coenzyme binding site (GSERSFQ) from chMDH [27], including the following six BsMDH mutants: BsMDH-T1a (S^{37}), BsMDH-T1b (R^{39}), BsMDH-T3($G^{36}S^{37}S^{40}$), pBsMDH-T4($G^{36}S^{37}R^{39}S^{40}$), pBsMDH-T5 ($G^{36}S^{37}R^{39}S^{40}Q^{42}$), pBsMDH-T7 ($G^{36}S^{37}E^{38}R^{39}S^{40}F^{41}Q^{42}$). The primers, plasmids and strains used for these mutations are listed in Supplementary Table S1. The mutants were constructed using overlap PCR, and then ligated to pET-28b(+) plasmid by double restriction endonuclease digestion, which were further transformed in the *E. coli* Rosetta BL21(DE3) pLysS. After validation by Sanger sequencing, a positive clone was subjected for protein expression and purification as described above. In order to further verify whether the mutations on the coenzyme binding sites changed the secondary structure of MDH proteins, Circular Dichroism assays of wild-type and mutated MDHs were performed using a Circular Dichroism spectrometer (Tokyo, Japan). Finally, the kinetic parameters of mutated enzymes were determined using the methods described above.

3 Results

3.1 BsMDH Gene Sequence and Protein Expression

The full length BsMDH was 939 bp, encoding 312 amino acid residues. SDS–PAGE revealed a clear band at approximately 35 kDa (Fig. 1A). The result of gel filtration chromatography showed that the molecular weight of the target protein was approximately 74 kDa (Fig. 1B). After removing the his_6-tag, the native PAGE image showed two bands (Supplementary Fig. S1). The MALDI-TOF MS results showed two peaks with molecular masses of 68,988.36 and 34,532.4 Da (Fig. 1C), suggesting that BsMDH in the solution might form homodimers (69.0 kDa) with the molecular weight of each subunit of 34.5 kDa. The GPC-MALS analysis showed the molecular weight of the main

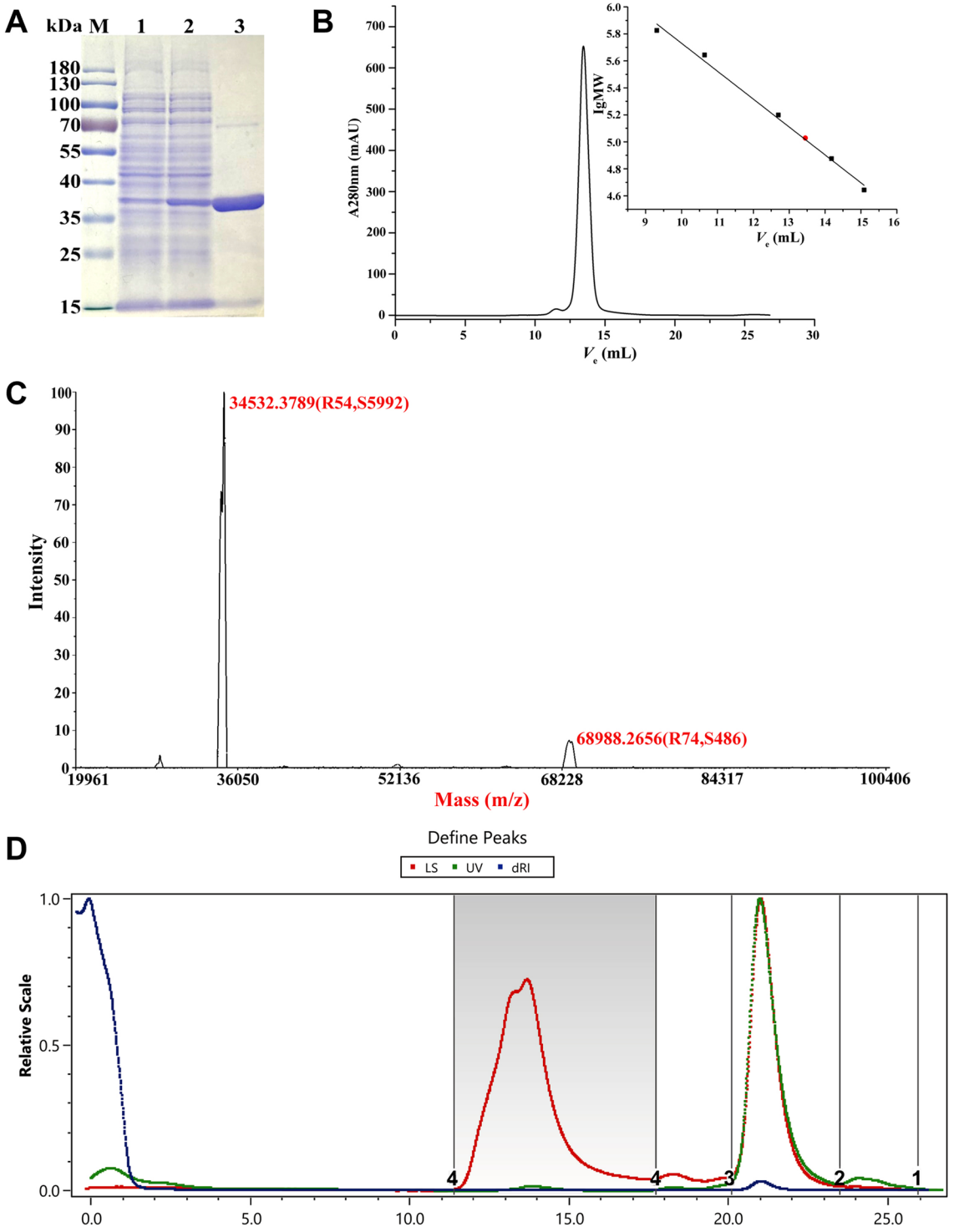

Fig. 1 Enzymatic properties of the recombinantly expressed BsMDH. **A** SDS–PAGE analysis. M: protein molecular weight marker. Lane 1: crude extracts of pET-28b(+) cells. Lane 2: crude extracts of cells transformed with BsMDH. Lane 3: purified BsMDH. **B** Gel filtration chromatography analysis. The standard curve shows the logarithmic molecular weight against elution volume. BsMDH was represented by the red circle. **C** MALDI-TOF-MS analysis of BsMDH without his_6-tag. Two single-charged molecular ions were observed at 34532.2789, and 68988.2656 Da. BSA was used as the external standard. R means resolution, and the S means the signal to noise ratio. **D** Gel Permeation Chromatography coupled to Multi-Angle Light Scattering (GPC-MALS) analysis of the oligomerization state of BsMDH without his_6-tag. LS (red): light scattering detector. UV (green): ultraviolet detector. dRI (blue): differential refractive index detector. Peak 2 at retention time from 20.105 min to 23.497 min was the major peak (93%), displaying Mw of 123.1 (±1.653%) kDa, and Mz of 133.0 (±4.023%) kDa (Color figure online)

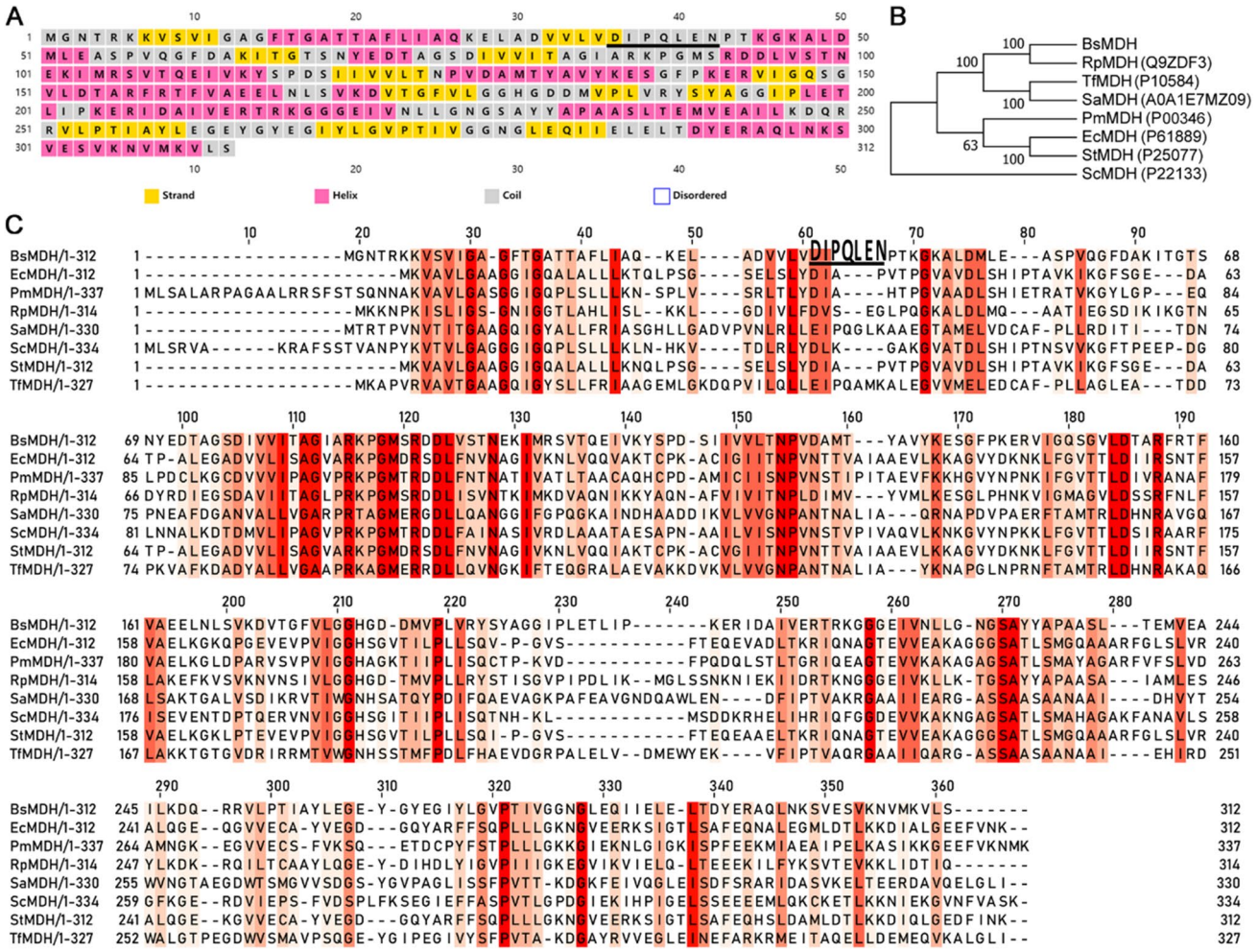

Fig. 2 Sequence features of the BsMDH. **A** Secondary structure prediction of BsMDH. **B** Neighbor-joining phylogenetic tree of MDH amino acid sequences. Percentage bootstrap values above 50 are shown at the branch nodes. **C** Alignment of MDH protein sequences. The red color represents the conservation degree at each site. The accession numbers for the sequences in uniport database are as follows: EcMDH, *Escherichia coli* strain K12, P61889; PmMDH, pig mitochondria, P00346; RpMDH, *Rickettsia prowazekii* strain Madrid E, Q9ZDF3; SaMDH, *Streptomyces aureofaciens*, A0A1E7MZ09; ScMDH, *Saccharomyces cerevisiae* strain S288c, P22133; StMDH, *Salmonella typhimurium* strain LT2, P25077; TfMDH, *Thermus flavus* AT-62/*Thermus thermophilus* ATCC 33923, P10584 (Color figure online)

peak (peak 2, 93.0%) was 123.1 ± 1.653% kDa (Fig. 1D), suggesting that the forms of BsMDH in the solution of GPC-MALS might be a mixture of homodimers and homotetramers. Overall, these data suggested that BsMDH might form dimers or tetramers in different buffer systems.

The secondary structure of BsMDH was predicted to contain 13 strands, 11 helixes and 23 coils (Fig. 2A). The phylogenetic analysis revealed that BsMDH was clustered with MDHs from Gram-positive and Gram-negative bacteria but isolated from eukaryotes (Fig. 2B). Alignment of protein sequences revealed that the NAD^+ coenzyme binding site (D^{36}IPQLEN^{42}, Fig. 2C with black underline) was localized to a relatively less conservative area.

3.2 Effects of pH and Temperature on Enzyme Activity

Along with increasing temperature and pH, BsMDH activity increased from 20 to 38 °C and from pH 7.0 to 8.0, but then decreased. The optimal pH and temperature for BsMDH activity were 8.0 and 38 °C, respectively (Fig. 3A, B).

As shown in Fig. 3C, the residual activity of BsMDH maintained above 75% after treated at 30–40 °C for 20 min. When the temperature was above 40 °C, the residual enzyme activity of BsMDH decreased sharply with the gradually increased temperature. The residual activity was less than 20% of the initial enzyme activity after treatment at 55 °C for 20 min.

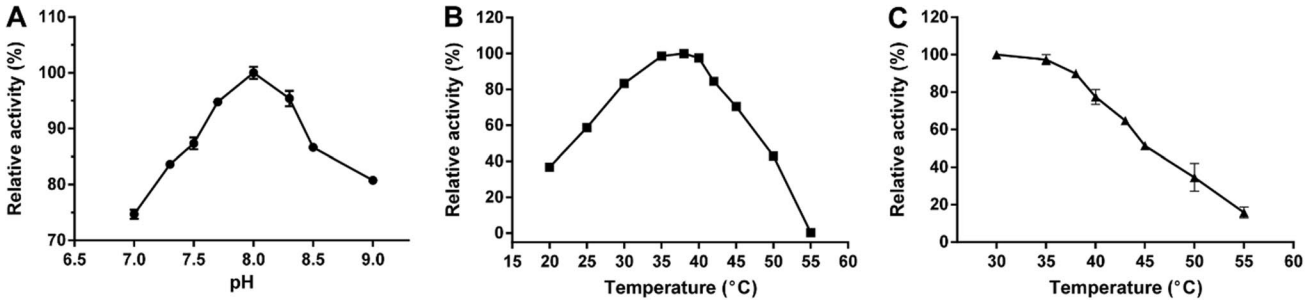

Fig. 3 Effects of temperature and pH on the activity of recombinant BsMDH (mean ± SD).**A** Effects of pH on the activity of recombinant BsMDH. **B** Effects of temperature on the activity of recombinant BsMDH. **C** Effects of temperature on the stability of recombinant BsMDH

Table 1 Effects of metal ions on the recombinant BsMDH activity

Metal ions	Relative activity (%)	Metal ions	Relative activity (%)
None	100.00	2 mM Co^{2+}	17.90 ± 1.01
2 mM Mg^{2+}	90.20 ± 3.83	2 mM Cu^{2+}	17.44 ± 0.32
2 mM Ca^{2+}	69.39 ± 1.43	2 mM K^{+}	12.09 ± 1.55
2 mM Mn^{2+}	62.04 ± 0.25	2 mM Na^{+}	3.28 ± 0.70
2 mM Ni^{2+}	52.16 ± 4.07	2 mM Rb^{+}	0.00 ± 0.00
2 mM Zn^{2+}	18.62 ± 0.44	2 mM Li^{+}	0.00 ± 0.00

Values are expressed as mean ± standard deviation

Table 2 Effects of small organic compounds on the activity of the recombinantly expressed BsMDH

Compounds	Relative activity (%)
None	100.00
2 mM α-KG	83.37 ± 2.1
2 mM DTT	93.12 ± 0.55
5 mM DTT	84.88 ± 0.82
2 mM EDTA	91.62 ± 1.48
5 mM EDTA	98.41 ± 2.05
2 mM ATP	98.04 ± 1.18
2 mM ADP	75.46 ± 1.64
2 mM AMP	54.29 ± 1.17

Values are expressed as mean ± standard deviation

α-KG α-ketoglutaric acid, *DTT* dithiothreitol, *EDTA* ethylene diamine tetraacetic acid, *ATP* adenosine triphosphate, *ADP* adenosine diphosphate, *AMP* adenosine monophosphate

3.3 Effects of Metal Ions and Metabolic Reagents on BsMDH Activity

Treatments with 2 mM Rb^{+}, Na^{+} and Li^{+} almost completely inhibited BsMDH enzyme activity. The activity of BsMDH decreased over 80% in the presence of 2 mM Co^{2+}, Zn^{2+}, Cu^{2+} and K^{+}. Other metal ions at the concentration of 2 mM such as Mn^{2+}, Mg^{2+}, Ca^{2+}, and Ni^{2+} also exhibited inhibitory activities on BsMDH activity, with the inhibitory rates ranging from 10 to 88%. These results indicated that BsMDH might be a metallic-ion-independent dehydrogenase, and its activity was inhibited by various metal ions (Table 1).

Regarding the effects of small molecular compounds, addition of 2 mM ATP, ADP and AMP inhibited BsMDH activity. Especially the addition of AMP inhibited almost 46% of BsMDH activity. Other small metabolic compounds, including α-KG, DTT and EDTA, slightly inhibited BsMDH activity, and the residual activity still maintained above 80% (Table 2).

3.4 Kinetic Parameters of BsMDH

As shown in Table 3, and Supplementary Fig. S2, K_m and k_{cat} of NADH were 54.97 μM and 86.10 s^{-1}, respectively, and those of NADPH were 573.3 μM and 3.85 s^{-1}, respectively. The catalytic efficiency (k_{cat}/K_m) values of BsMDH for NADH and NADPH were 1.57 μM^{-1} s^{-1} and 0.007 μM^{-1} s^{-1}, respectively. The K_m value for OAA was 970.8 μM, and its catalytic efficiency (k_{cat}/K_m) was 0.32 μM^{-1} s^{-1} (Table 4, Supplementary Fig. S2).

3.5 Kinetic Analysis of Mutated Enzymes

Totally, six mutants on the key coenzyme binding site of BsMDH were constructed. The Circular Dichroism analysis showed that the curves of mutated proteins were basically consistent with that of the wild-type BsMDH (Supplementary Fig. S3), indicating that mutations at these sites did not significantly affect their secondary structure.

The K_m values for NADH (K_m^{NADH}) and NADPH (K_m^{NADPH}) of the six mutants are listed in Table 5. Among them, the preference of BsMDH-T5 to NADPH was five times higher than to NADH, and coenzyme specificity to NADH of this mutant reduced from 224.3 to 0.2 (1122 folds). The coenzyme specificity of BsMDH-T7 to NADPH was 2039 folds higher than that of BsMDH, indicating the

Table 3 Kinetic parameters of BsMDH and MDHs from other organisms

Enzyme	NADH			NADPH			Specificity	References
	K_m (μM)	k_{cat} (s^{-1})	k_{cat}/K_m (A) (μM^{-1} s^{-1})	K_m (μM)	k_{cat} (s^{-1})	k_{cat}/K_m (B) (μM^{-1} s^{-1})	A/B	
BsMDH	54.97	86.10	1.57	573.3	3.85	0.007	224.3	This study
BaMDH	14.0	78.7	5.62	130	9.4	0.072	78.06	[29]
ScMDH	82.58	542	6.56	1106.5	36.07	0.033	198.89	[30]
TfMDH	3.05	259.2	84.98	42.13	164.4	3.88	21.90	[35]

BsMDH Bacillus subtilis MDH in this study, *BaMDH* MDH from *Bacillus* sp., *ScMDH* MDH from *Saccharomyces cerevisiae*, *TfMDH* MDH from *Thermus flavus*

Table 4 Kinetic parameters of BsMDH for different substrates

Substrate	K_m (μM)	k_{cat} (s^{-1})	k_{cat}/K_m (μM^{-1} s^{-1})
OAA	970.8	307.21	0.32
malate	285.7	27.23	0.095
NAD^+	176.8	35.17	0.20

OAA oxaloacetate

complete conversion of coenzyme specificity after mutation of certain amino acids. Notably, the other mutants, including BsMDH-T3, and BsMDH-T4, also showed great changes of k_{cat}/K_m, when the coenzyme changed from NADH to NADPH, with the degree of alteration of 329, and 575 folds, respectively.

4 Discussion

As previously reported, MDHs from *Bacillus* were predicted to be homotetramer based on the molecular mass analyses, including *B. caldotenax* [28], *B. subtilis* [29], and *B. stearothermophilus* [30]. Monomer state of MDH was also reported from another *B. subtilis* strain [29]. In addition, Wynne *et al.* [30] reported that the MDH from *B. stearothermophilus* could form dimers when the pH decreased below 3.5 but tetramer at pH higher than 3.5. Inconsistent with these results, in this study, both gel filtration and MALDI-TOF MS analyses indicated that BsMDH with his_6-tag could form homodimer at pH 8.0. In addition, native-PAGE revealed two bands of BsMDH without his_6-tag. MALDI-TOF MS analyses also revealed that BsMDH without his_6-tag formed dimers. The GPC-MALS analysis revealed that the molecular weight of BsMDH was 123.1 kDa, which might be a mixture of dimer and tetramer. These results suggested that, in addition to tetramer, BsMDH might also form dimer, which is a novel finding and extends our knowledge on the oligomerization diversity of this enzyme. The inconsistent results between MALDI-TOF MS and GPC-MALS might be due to the different buffer systems, which required further investigations.

For the recombinantly expressed BsMDH, the k_{cat}/K_m value of OAA (0.32 μM^{-1} s^{-1}) was higher than that of malate (0.095 μM^{-1} s^{-1}), and the k_{cat}/K_m value of NADH (1.57 μM^{-1} s^{-1}) was higher than that of NAD^+ (0.20 μM^{-1} s^{-1}). These results indicated that BsMDH might be more efficient to catalyze the reaction from OAA to malate than the reverse direction, which would benefit to the industrial synthesis of malate.

For enzymatic properties, the optimum pH for BsMDH activity was approximately 8.0, which was similar to MDH from *Streptomyces aureofaciens* (SaMDH) and MDH from *Saccharomyces cerevisiae* (ScMDH) [31, 32]. The thermal stability of MDHs was generally low, which could be improved by the increased number of hydrogen or disulfide bonds. Compared with MDHs of other species, thermophilic MDHs had more hydrogen bonds between the protein subunits of polar amino acid residues [33, 34]. MDHs from thermophilic microorganisms, i.e. ScMDH and NeMDH could retain most activity after treatment at 50 °C, but were completely inactivated after treatment at 60 °C [31, 35]. In the present study, BsMDH could retain approximately 75% of activity after treatment at 40 °C, but less than 20% of activity at 55 °C, indicating a moderate thermal stability of BsMDH. Comparison between different MDHs revealed that the affinity of thermophilic tetramer BaMDH (MDH from *Bacillus* sp.) to NADH and NADPH was higher than that of BsMDH (K_m value), but the specificity of BsMDH to NADH was 2.87 times higher than those of BaMDH, ScMDH and TfMDH (MDH from *Thermus flavus*) [27, 30, 31] (Table 3).

Generally, the normal function of MDHs does not require metal ions. However, its activity may be affected by metal ions. The reductive activity of MDHs was inhibited by TCA cycle metabolites, such as excess oxaloacetate and divalent metal ions [5, 36]. In general, Ca^{2+}, Mg^{2+} and most small molecular compounds did not greatly affect, but Zn^{2+} exhibited significant inhibitory effects on *Phaseolus mungo* MDH activity [37]. In the present study, similar results were observed. In contrast, K^+, Co^{2+} and Ni^{2+}

Table 5 Kinetic parameters of the recombinant BsMDH and its mutants

Enzyme	NADH			NADPH			A/B	B/A	Degree of alteration
	K_m (μM)	k_{cat} (s^{-1})	k_{cat}/K_m (A) ($\mu M^{-1}\ s^{-1}$)	K_m (μM)	k_{cat} (s^{-1})	k_{cat}/K_m (B) ($\mu M^{-1}\ s^{-1}$)			
BsMDH	54.97	86.10	1.57	573.3	3.92	0.007	224.3	0.004	1.00
BsMDH-T1a	51.98	130.47	2.51	398.1	21.33	0.05	50.2	0.02	4.47
BsMDH-T1b	76.12	63.05	0.83	205.8	14.16	0.07	11.9	0.08	18.85
BsMDH-T3	98.44	177.32	1.80	124.2	326.96	2.63	0.68	1.46	329.85
BsMDH-T4	196.3	120.84	0.62	84.64	133.93	1.58	0.39	2.55	575.13
BsMDH-T5	232.4	116.42	0.50	49.37	37.22	2.48	0.2	4.96	1121.50
BsMDH-T7	255.9	140.60	0.55	23.8	122.41	5.14	0.11	9.35	2039.09

A represents k_{cat}/K_m of NADH, *B* represents k_{cat}/K_m of NADPH

significantly promoted the activity of most MDH enzymes [36], but inhibited the activity of BsMDH in the present study. The underlying reasons were unknown and required further investigations.

α-KG, ATP, ADP and AMP are general metabolites in cells. DTT, and EDTA are commonly used components in buffer systems. Effects of these chemicals on BsMDH activity should be important for industrial application of BsMDH. As reported, rat MDH was inhibited by α-KG [38]. Activity of mitochondrial MDH from *Arabidopsis thaliana* was inhibited by AMP, ADP, and ATP, among which ATP showed the strongest inhibition [39]. Similar results were also observed in mitochondrial MDH from *Solanum tuberosum* [40]. Moreover, MDH activity from bacterium *Nitrosomonas europaea* was not strongly activated or inhibited by adenine nucleotides [26]. In the present study, α-KG, ADP and AMP showed remarkable inhibition to BsMDH. These results were consistent with the above publications, suggesting that application of BsMDH should avoid contamination of these molecules. In addition, DTT revealed moderate inhibition to BsMDH, probably due to the effects of DTT on disulfide bonds between BsMDH monomers, which are important to form dimers or tetramers.

As the k_{cat}/K_m values showed, in the presence of NADH, the catalytic efficiency of wide-type BsMDH was much higher than that using NADPH as the coenzyme, suggesting BsMDH relied on NADH as the coenzyme. This result was consistent with the most published bacterial MDHs [5]. As reported, only chloroplast MDHs were NADPH-dependent, while other MDHs, including LDH-like MDH, were NADH-dependent. Further tests of six mutated BsMDHs showed clear switch of coenzyme preference from NADH to NADPH, especially BsMDH-T5 and BsMDH-T7, displaying the degrees of alteration (the ratio of $k_{cat}/K_m{}^{NADH}$ of mutated enzyme to the $k_{cat}/K_m{}^{NADPH}$ of wide type) of 1121 and 2039 times, respectively. NADPH-dependent MDHs have been identified in nature. However, BsMDH-T7 generated in the present study revealed a lower K_m value than wide-type NADPH-dependent MDHs from *Thermus flavus* (TfMDH), *Corynebacterium glutamicum* (CgMDH), *Sorghum vulgare* leaf chloroplasts (chMDH(SV)) and *Zea mays* chloroplasts (chMDH(ZM)). In addition, BsMDH-T7 showed higher k_{cat} and k_{cat}/K_m values to NADPH than those of TfMDH and CgMDH, but lower than chMDH(SV) [27, 41–44] (Table 6). These results indicate that the created BsMDH-T7 mutant is a novel NADPH-dependent enzyme, which displayed better catalytic parameters than the reported NADPH-dependent MDHs, and might be potentially applied in industrial production.

As reported on dehydrogenase, cofactor binding sites are associated with arginine mutations [45, 46]. Similarly, in the present study, mutation on R^{39} (BsMDH-T1b) showed a degree of alteration of 4.47 in comparison to the wide type, and mutations on $G^{36}S^{37}R^{39}S^{40}$ (pBsMDH-T4) showed a higher degree of alteration than BsMDH-T3($G^{36}S^{37}S^{40}$), both indicating that R^{39} might be an important site for coenzyme preference. Arginine could interact with the 2′-phosphate group of adenine ribose of NADPH. In addition, replacement of Asp^{36} by Gly revealed promotive effects on preference switch from NADH to NADPH, probably due to the disappearance of electrostatic repulsion to NADPH and steric hindrance reported in several dehydrogenase [43, 47].

In summary, BsMDH may form both dimer and tetramer in vitro, depending on the buffer system. The optimum temperature and pH of BsMDH were 38 °C and pH 8.0, respectively. BsMDH shows a moderate thermal stability, and a higher efficacy in the catalysis direction of malate synthesis than the reverse. Mutations of certain amino acids at the coenzyme specific binding site change the coenzyme preference of BsMDH from NADH to NADPH. Among the mutants, BsMDH-T7 revealed a relatively lower K_m value, but relatively higher k_{cat} and k_{cat}/K_m than TfMDH and CgMDH. Overall, these results suggest that BsMDH and

Table 6 Comparison of the enzymatic kinetic parameters of NADPH-dependent mutated BsMDHs in this study and wild-type NADPH-dependent MDHs from other organisms

Enzyme	NADH			NADPH			References
	K_m (μM)	k_{cat} (s^{-1})	k_{cat}/K_m (A) (μM^{-1} s^{-1})	K_m (μM)	k_{cat} (s^{-1})	k_{cat}/K_m (B) (μM^{-1} s^{-1})	
BsMDH	54.97	86.10	1.57	573.3	3.92	0.007	This study
BsMDH-T3	98.44	177.32	1.80	124.2	326.96	2.63	This study
BsMDH-T4	196.3	120.84	0.62	84.64	133.93	1.58	This study
BsMDH-T5	232.4	116.42	0.50	49.37	37.22	2.48	This study
BsMDH-T7	255.9	140.60	0.55	23.8	122.41	5.14	This study
TfMDH	3.05	259.2	84.92	42.13	164.4	3.9	[35]
CgMDH	7	2	2.8	25	2.8	1.12	[38]
mtMDH II	90	–	–	20	–	–	[39]
chMDH(SV)		–	–	40	630	17	[40]
chMDH(ZM)	830	–	–	24	–	–	[41]

TfMDH Thermus flavus MDH, *CgMDH Corynebacterium glutamicum* MDH, *chMDH(SV)* MDH of *Sorghum vulgare* leaf chloroplasts, *chMDH(ZM)* MDH of *Zea mays* chloroplasts, *MjMDH* MDH of *Methanococcus jannaschii*

its mutant BsMDH-T7 are promising enzymes for malate production.

Supplementary Information The online version contains supplementary material available at https://doi.org/10.1007/s10930-022-10087-0.

Acknowledgements We would like to thank professor Guo-Ping Zhu (College of Life Sciences, Anhui Normal University, China), Anhui Provincial Key Laboratory of the Conservation and Exploitation of Biological Resources, Anhui Provincial Key Laboratory of Molecular Enzymology and Mechanism of Major Diseases, Key Laboratory of Biomedicine in Gene Diseases and Health of Anhui Higher Education Institutes for excellent technical support.

Author Contributions YDG designed the experiments. FZS, LLJ and SLH collected samples, performed the comparative genomic analysis and analyzed the data. HHW and YTG drafted the manuscript and all authors revised it.

Funding This work was supported by the National Natural Science Foundation of China [Grant Nos. 31300006, 32070463].

Data Availability All data have been included in the manuscript and supplementary materials.

Declarations

Conflict of interest The authors declare no conflicts of interest.

References

1. Rudrappa T, Czymmek KJ, Paré PW, Bais HP (2008) Root-secreted malic acid recruits beneficial soil bacteria. Plant Physiol 148(3):1547–1556
2. Gietl C (1992) Malate dehydrogenase isoenzymes: cellular locations and role in the flow of metabolites between the cytoplasm and cell organelles. Biochim Biophys Acta 1100(3):217–234
3. Meyer FM, Gerwig J, Hammer E, Herzberg C, Commichau FM, Völker U, Stülke J (2011) Physical interactions between tricarboxylic acid cycle enzymes in *Bacillus subtilis*: evidence for a metabolon. Metab Eng 13(1):18–27
4. Swinnen IA, Bernaerts K, Dens EJ, Geeraerd AH, Van Impe JF (2004) Predictive modelling of the microbial lag phase: a review. Int J Food Microbiol 94(2):137–159
5. Takahashi-Íñiguez T, Aburto-Rodríguez N, Vilchis-González AL, Flores ME (2016) Function, kinetic properties, crystallization, and regulation of microbial malate dehydrogenase. J Zhejiang Univ Sci B 17(4):247–261
6. Harrison JF, Nielsen DI, Page R (1996) Malate dehydrogenase phenotype, temperature and colony effects on flight metabolic rate in the honey-bee, *Apis mellifera*. Funct Ecol 10(1):81–88
7. Liu Z, Yuan F, Yang Y, Yin L, Liu Y, Wang Y, Zheng K, Cao J (2016) Partial protective immunity against toxoplasmosis in mice elicited by recombinant *Toxoplasma gondii* malate dehydrogenase. Vaccine 34(7):989–994
8. Thakker C, Martínez I, Li W, San K-Y, Bennett GN (2015) Metabolic engineering of carbon and redox flow in the production of small organic acids. J Ind Microbiol Biotechnol 42(3):403–422
9. Dong X, Chen X, Qian Y, Wang Y, Wang L, Qiao W, Liu L (2017) Metabolic engineering of *Escherichia coli* W3110 to produce L-malate. Biotechnol Bioeng 114(3):656–664
10. Geiser DM, Pitt JI, Taylor JW (1998) Cryptic speciation and recombination in the aflatoxin-producing fungus *Aspergillus flavus*. Proc Natl Acad Sci USA 95(1):388–393
11. Zhang X, Wang X, Shanmugam KT, Ingram LO (2011) L-Malate production by metabolically engineered *Escherichia coli*. Appl Environ Microbiol 77(2):427–434
12. Mu L, Wen J (2013) Engineered *Bacillus subtilis* 168 produces L-malate by heterologous biosynthesis pathway construction and lactate dehydrogenase deletion. World J Microbiol Biotechnol 29(1):33–41
13. Lin P, Yuan H, Du J, Liu K, Liu H, Wang T (2020) Progress in research and application development of surface display technology using *Bacillus subtilis* spores. Appl Microbiol Biotechnol 104(6):2319–2331
14. Karpov DS, Domashin AI, Kotlov MI, Osipova PG, Kiseleva SV, Seregina TA, Goncharenko AV, Mironov AS, Karpov VL, Poddubko SV (2020) Biotechnological potential of the *Bacillus subtilis* 20 strain. Mol Biol 54(1):119–127

15. Kunst F et al (1997) The complete genome sequence of the Gram-positive bacterium *Bacillus subtilis*. Nature 390(6657):249–256
16. Lee NK, Kim WS, Paik HD (2019) *Bacillus* strains as human probiotics: characterization, safety, microbiome, and probiotic carrier. Food Sci Biotechnol 28(5):1297–1305
17. Olmos J, Acosta M, Mendoza G, Pitones V (2020) *Bacillus subtilis*, an ideal probiotic bacterium to shrimp and fish aquaculture that increase feed digestibility, prevent microbial diseases, and avoid water pollution. Arch Microbiol 202(3):427–435
18. Romero-Garcia S, Hernández-Bustos C, Merino E, Gosset G, Martinez A (2009) Homolactic fermentation from glucose and cellobiose using *Bacillus subtilis*. Microb Cell Fact 8(1):23
19. Kleijn RJ, Buescher JM, Le Chat L, Jules M, Aymerich S, Sauer U (2010) Metabolic fluxes during strong carbon catabolite repression by malate in *Bacillus subtilis*. J Biol Chem 285(3):1587–1596
20. Stülke J, Hillen W (2000) Regulation of carbon catabolism in *Bacillus* species. Annu Rev Microbiol 54:849–880
21. Lu Y, Mei L (2007) Co-expression of P450 BM3 and glucose dehydrogenase by recombinant *Escherichia coli* and its application in an NADPH-dependent indigo production system. J Ind Microbiol Biotechnol 34(3):247–253
22. Kumar S, Stecher G, Tamura K (2016) MEGA7: molecular evolutionary genetics analysis version 7.0 for bigger datasets. Mol Biol Evol 33(7):1870–1874
23. Thompson JD, Higgins DG, Gibson TJ (1994) CLUSTAL W: improving the sensitivity of progressive multiple sequence alignment through sequence weighting, position-specific gap penalties and weight matrix choice. Nucleic Acids Res 22(22):4673–4680
24. Ge YD, Jiang LL, Hou SL, Su FZ, Wang P, Zhang G (2020) Heteroexpression and biochemical characterization of thermostable citrate synthase from the cyanobacteria *Anabaena* sp. PCC7120. Protein Expr Purif 168:105565
25. Maloney AP, Callan SM, Murray PG, Tuohy MG (2004) Mitochondrial malate dehydrogenase from the thermophilic, filamentous fungus *Talaromyces emersonii*. Eur J Biochem 271(15):3115–3126
26. Deutch CE (2013) L-Malate dehydrogenase activity in the reductive arm of the incomplete citric acid cycle of *Nitrosomonas europaea*. Antonie Van Leeuwenhoek 104(5):645–655
27. Nishiyama M, Birktoft JJ, Beppu T (1993) Alteration of coenzyme specificity of malate dehydrogenase from *Thermus flavus* by site-directed mutagenesis. J Biol Chem 268(7):4656–4660
28. Smith K, Sundaram TK, Kernick M (1984) Malate dehydrogenases from actinomycetes: structural comparison of *Thermoactinomyces* enzyme with other actinomycete and *Bacillus* enzymes. J Bacteriol 157(2):684–687
29. Sundaram TK, Wright IP, Wilkinson AE (1980) Malate dehydrogenase from thermophilic and mesophilic bacteria. Molecular size, subunit structure, amino acid composition, immunochemical homology, and catalytic activity. Biochemistry 19(10):2017–2022
30. Wynne SA, Nicholls DJ, Scawen MD, Sundaram TK (1996) Tetrameric malate dehydrogenase from a thermophilic *Bacillus*: cloning, sequence and overexpression of the gene encoding the enzyme and isolation and characterization of the recombinant enzyme. Biochem J 317:235–245
31. Ge YD, Cao ZY, Wang ZD, Chen LL, Zhu YM, Zhu GP (2010) Identification and biochemical characterization of a thermostable malate dehydrogenase from the mesophile *Streptomyces coelicolor* A3(2). Biosci Biotechnol Biochem 74(11):2194–2201
32. Labrou NE, Clonis YD (1997) L-Malate dehydrogenase from *Pseudomonas stutzeri*: purification and characterization. Arch Biochem Biophys 337(1):103–114
33. Bjørk A, Dalhus B, Mantzilas D, Eijsink VG, Sirevåg R (2003) Stabilization of a tetrameric malate dehydrogenase by introduction of a disulfide bridge at the dimer–dimer interface. J Mol Biol 334(4):811–821
34. Jaindl M, Popp M (2006) Cyclitols protect glutamine synthetase and malate dehydrogenase against heat induced deactivation and thermal denaturation. Biochem Biophys Res Commun 345(2):761–765
35. Yoshida A (1965) Purification and chemical characterization of malate dehydrogenase of *Bacillus subtilis*. J Biol Chem 240:1113–1117
36. Takeya M, Ito S, Sukigara H, Osanai T (2018) Purification and characterisation of malate dehydrogenase from *Synechocystis* sp. PCC 6803: biochemical barrier of the oxidative tricarboxylic acid cycle. Front Plant Sci 9:947
37. Wang S, Xu Z, Ye X, Rao P (2005) Purification and characterization of a malate dehydrogenase from *Phaseolus mungo*. J Food Biochem 29(2):117–131
38. Fahien LA, Kmiotek EH, Macdonald MJ, Fibich B, Mandic M (1988) Regulation of malate dehydrogenase activity by glutamate, citrate, alpha-ketoglutarate, and multienzyme interaction. J Biol Chem 263(22):10687–10697
39. Yoshida K, Hisaboria T (2016) Adenine nucleotide-dependent and redox-independent control of mitochondrial malate dehydrogenase activity in *Arabidopsis thaliana*. Biochim Biophys Acta 1857(6):810–818
40. Rustin P, Valat M (1986) The control of malate dehydrogenase activity by adenine nucleotides in purified potato tuber (*Solanum tuberosum* L.) mitochondria. Arch Biochem Biophys 247(1):62–67
41. Genda T, Nakamatsu T, Ozak H (2003) Purification and characterization of malate dehydrogenase from *Corynebacterium glutamicum*. J Biosci Bioeng 95(6):562–566
42. Thompson H, Tersteegen A, Thauer RK, Hedderich R (1998) Two malate dehydrogenases in *Methanobacterium thermoautotrophicum*. Arch Microbiol 170(1):38–42
43. Lemaire M, Miginiac-Maslow M, Decottignies P (1996) The catalytic site of chloroplastic NADP-dependent malate dehydrogenase contains a His/Asp pair. Eur J Biochem 236(3):947–952
44. Kagawa T, Bruno PL (1988) NADP-malate dehydrogenase from leaves of *Zea mays*: purification and physical, chemical, and kinetic properties. Arch Biochem Biophys 260(2):674–695
45. Ashton AR, Trevanion SJ, Carr PD, Verger D, Ollis DL (2000) Structural basis for the light regulation of chloroplast NADP malate dehydrogenase. Physiol Plant 110(3):314–321
46. Birktoft JJ, Banaszak LJ (1983) The presence of a histidine-aspartic acid pair in the active site of 2-hydroxyacid dehydrogenases. X-ray refinement of cytoplasmic malate dehydrogenase. J Biol Chem 258(1):472–482
47. Chakraborty J, Nemeria NS, Farinas E, Jordan F (2018) Catalysis of transthiolacylation in the active centers of dihydrolipoamide acyltransacetylase components of 2-oxo acid dehydrogenase complexes. FEBS Open Bio 8(6):880–896